

Pore size control through benzene vapor deposition on activated carbon

Hyun Uk Kang, Wun-gwi Kim, Sung Hyun Kim*

Department of Chemical & Biological Engineering, Korea University, 5-1 Anam-dong,
Sungbuk-Ku, Seoul 136-701, South Korea

Received 30 August 2006; received in revised form 5 December 2006; accepted 13 January 2008

Abstract

Carbon adsorbents are considered as prime material to separate oxygen and nitrogen in PSA process. It is known that selectivity of carbon adsorbents can be added by adjusting pore size on the adsorbents. Among many treatment methods, chemical vapor deposition method was selected and benzene was used as a chemical agent. Activated carbons were heated at 5 °C/min and 10 °C/min in inert condition. The peak temperature at 700 °C and 800 °C was maintained while activated carbons were treated with benzene vapor. Inert condition was given as laminar and turbulent flow conditions.

Pore size distribution results investigated by adsorption of various gases including CO₂ (3.3 Å), *n*-butane (4.3 Å) and *iso*-butane (5.0 Å), assured of the pore constriction or heightened energy barrier on the pore opening. The nitrogen diffusivity and the selectivity of treated samples are inversely proportioned. That means selectivity comes out, when pore mouth is well blocked, not to admit the nitrogen molecules.

© 2008 Elsevier B.V. All rights reserved.

Keywords: Activated carbon; Chemical vapor deposition; Adsorption; Diffusion

1. Introduction

Carbon molecular sieves (CMS) are considered as prime material in PSA process for its rapid adsorption/desorption rate and large adsorption capacity. It is known that selectivity of carbon adsorbents comes from controlled pore size distribution (PSD). Carbon molecular sieves can be made from activated carbons by various post treatments [1,2]. Many researchers invented various methods to narrow pores of the adsorbents which have been prepared by pyrolysis of synthetic and natural precursors [3–5]. Among those, chemical vapor deposition (CVD) method turns out to be the major one to control its pore size [6–8]. There have been several reports regarding control of pores in active carbon using CVD techniques [9–11]. Previous works by other researchers showed the coke treatment with a carbonaceous substance to deposit hydrocarbon from 600 °C to 900 °C and narrow the pores present in the coke. Carbonaceous substances that can be used in the treatments include benzene, ethylene, ethane, hexane, cyclohexane, methanol and *iso*-butylene [12–15]. Upon pyrolysis, carbon molecules are deposited and modify the pore structure of the base carbonaceous materials, thus improving its separation ability for oxygen from air.

The main factors of the CMS are the adsorption ability, the selectivity, and the pore size distribution. To control them, the control of the properties of base materials is important as much as the control of PSA process because there are many types of active carbon and their properties will be changed by the treating condition. The target of this study is to gather information about CVD method as a post treatment to control pore size on the base materials. In addition to the process variables, more deep understanding of the pore structure of the treated materials could help exact establishment in process condition. Common method to investigate pore size distributions of adsorbents is BET adsorption analysis, but in case of carbon molecular sieves, 77 K nitrogen adsorption cannot be occurred and the pore size of it is not measured exactly. It is reported that indirect method to investigate pore size distribution of adsorbents by the adsorption of some gas molecules will help in understanding the pore structures on the adsorbents [2].

2. Theory

There are several attempts to explain the slower transport of nitrogen gas than oxygen gas into the carbon molecular sieve

* Corresponding author. Tel.: +82 2 3290 3297; fax: +82 2 926 6102.
E-mail address: kimsh@korea.ac.kr (S.H. Kim).

suitable for air separation process. Among those, the most proper theory to explain the adsorption kinetics is that gas diffuses rapidly into the macropore regions in the few initial seconds for there is little diffusion resistance by their broad pore sizes and then, diffuses into the micropores relatively slowly. If the adsorption isotherm is considered linear over the individual pressure step, such an adsorption and diffusion process may be represented by the dual diffusion model, discussed and summarized by Ruthven et al. [16].

In this model, the gas uptake curve is given by:

$$\frac{m_t}{m_\infty} = 1 - \frac{18}{\beta + 3\alpha} \sum_{m=1}^{\infty} \sum_{n=1}^{\infty} \left(\frac{n^2 \pi^2}{p_{n,m}^4} \right) \times \frac{\exp[-p_{n,m}^2 D_C t / r_C^2]}{\{\alpha + (\beta/2) [1 + (\cot(p_{n,m})/p_{n,m})(p_{n,m} \cot(p_{n,m}) - 1)]\}} \quad (1)$$

where, m_t is gas uptake at time t , m_∞ is gas uptake at equilibrium, D_C is diffusivity in micropore of microparticle, r_C is microparticle radius, α is dimensionless rate parameter, β is dimensionless parameter and $p_{n,m}$ is given by the roots of the equation

$$\alpha p_{n,m}^2 - n^2 \pi^2 = \beta(p_{n,m} \cot(p_{n,m}) - 1) \quad (2)$$

If α is small, β will also be small and the roots of Eq. (2) will approach $m\pi$ for all n ($p_{n,m} \rightarrow m\pi$). At these conditions, cotangent p is always large. Since $\sum_{n=1}^{\infty} (1/n^2 \pi^2) = 1/6$ and $p_m = m\pi$, Eq. (1) simplifies to:

$$1 - \frac{m_t}{m_\infty} = \frac{6}{1 + 3\alpha/\beta} \times \sum_{m=1}^{\infty} \frac{1}{m^2 \pi^2} \exp\left[-\frac{m^2 \pi^2 D_C t}{r_C^2}\right] \quad (3)$$

The right-hand side of Eq. (3) is the ordinary solution to the diffusion equation divided by the factor $(1 + 3\alpha/\beta)$, which represents the ratio of total particle capacity to micropore capacity and can be expressed as Eq. (4):

$$1 - \frac{m_t}{m_\infty} = \frac{1}{1 + 3\alpha/\beta} \quad (4)$$

where m' is the initial macropore capacity.

At long times, the higher terms of the summation in Eq. (3) become very small, and Eq. (3) simplifies to:

$$\frac{1 - m_t}{m_\infty} \approx \frac{6}{\pi^2(1 + 3\alpha/\beta)} \exp\left[-\frac{\pi^2 D_C t}{r_C^2}\right] \quad (5)$$

then, a plot of $\ln[1 - m_t/m_\infty]$ vs. t should approach a straight line of slope $-\pi^2 D_C/r_C^2$ and intercept $\ln[6/\pi^2(1+3\alpha/\beta)]$.

At short times, by using Eq. (4), Eq. (3) can be expressed as:

$$\frac{m_t - m'}{m_\infty - m'} = 1 - 6 \times \sum_{m=1}^{\infty} \frac{1}{m^2 \pi^2} \exp\left[-\frac{m^2 \pi^2 D_C t}{r_C^2}\right] \quad (6)$$

The solution to the Eq. (6) for short times is as follows:

$$\frac{m_t - m'}{m_\infty - m'} = 6 \left(\frac{D_C t}{r_C^2} \right)^{1/2} \left[\pi - 1/2 + 2 \sum_{m=1}^{\infty} \frac{\text{ierfc}(m r_C)}{(D_C t)^{1/2}} \right] - \frac{3 D_C t}{r_C^2} \quad (7)$$

For short times this approximates to:

$$\frac{m_t - m'}{m_\infty - m'} \approx \frac{6}{r_C} \sqrt{\frac{D_C t}{\pi}} \quad (8)$$

By using Eq. (4), the initial macropore capacity, m' in Eq. (8) can be substituted with the term, $(1 + 3\alpha/\beta)$ and then, Eq. (8) is expressed as the follows:

$$\frac{m_t}{m_\infty} \approx \frac{3\alpha/\beta}{1 + 3\alpha/\beta} + \frac{1}{1 + 3\alpha/\beta} \frac{6}{r_C} \sqrt{\frac{D_C t}{\pi}} \quad (9)$$

Thus in the initial region a plot of m_t/m_∞ vs. \sqrt{t} should be linear with intercept $(3\alpha/\beta)/(1+3\alpha/\beta)$ and slope $[6/(1+3\alpha/\beta)]\sqrt{D_C/\pi r_C^2}$.

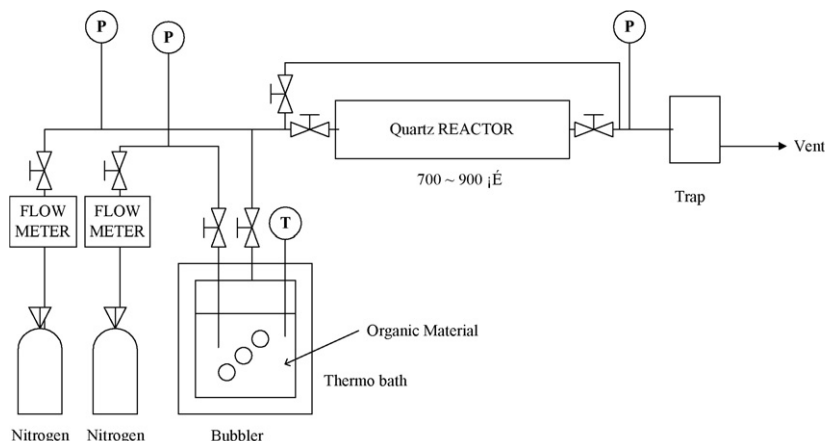


Fig. 1. Experimental apparatus for chemical vapor depositions.

By using this simple model, the highly accurate kinetic data of oxygen and nitrogen can be obtained.

3. Experimental

3.1. Chemical vapor deposition (CVD)

Activated carbon (SGF100, Samchully Company in Korea) based on coconut shell was used in this research. Benzene pyrolysis was performed by flowing a nitrogen stream containing 6 vol% benzene over the carbon material. Two types of nitrogen flow, the laminar and the turbulent flow were adopted. The sample was heated to 700 °C, 800 °C and 900 °C at a programmed rate of 5 °C/min and 10 °C/min. Then, benzene was supplied to the nitrogen flow for a fixed period of time. The chemical deposition amount was controlled by deposition time between 10 min and 50 min. For uniform deposition, loading cell was fixed in the tubular furnace and samples were on its base.

Tubular furnace and a bubbler to generate benzene vapor are the main parts in the CVD experiment. Fig. 1 shows the CVD equipment assembled for this experiment.

3.2. Adsorption procedure and apparatus

Adsorbents of three different types have been investigated; activated carbon (SGF100, Samchully Company in Korea), CMS made in Japan, and samples treated with CVD on activated carbon. Physical properties of activated carbon and CMS obtained by mercury porosimeter and BET experiment are

Table 1
Physical properties of activated carbon and CMS

	Activated carbon	Commercial CMS
Apparent density (g/cm ³)	1.0653	1.192
Total pore volume (ml/g)	0.6376	0.271
Average pore diameter	20.18	5.3
Specific surface area (m ² /g, BET)	1264	–

shown in Table 1. BET experiment was carried out on CMS, but adsorption could not be observed. Nitrogen adsorption experiment in 77 K showed that nitrogen was hard to be adsorbed on the CMS.

Adsorption of gases on activated carbon samples was carried out separately using a volumetric adsorption apparatus. Each sample was heated to 150 °C, maintained at 150 °C for 2 h and evacuated to desorb the organic compound and water on the adsorbents. The gas volumes adsorbed by the samples at a given initial pressure and temperature of 30 °C were determined from the change of pressure in the closed system.

The apparatus for adsorption experiment is composed of two main parts of the adsorption bed and the gas loading cylinder as in Fig. 2. Data acquisition computer gathered the signals from the pressure transmitter and temperature transmitter through analog-digital converter. When steady state occurred, the valve between adsorbent loading cell and gas cylinder closed and additional gas was loaded to the gas cylinder for next step. The adsorbent was characterized by BET method and adsorption of CO₂, *n*-butane and *iso*-butane.

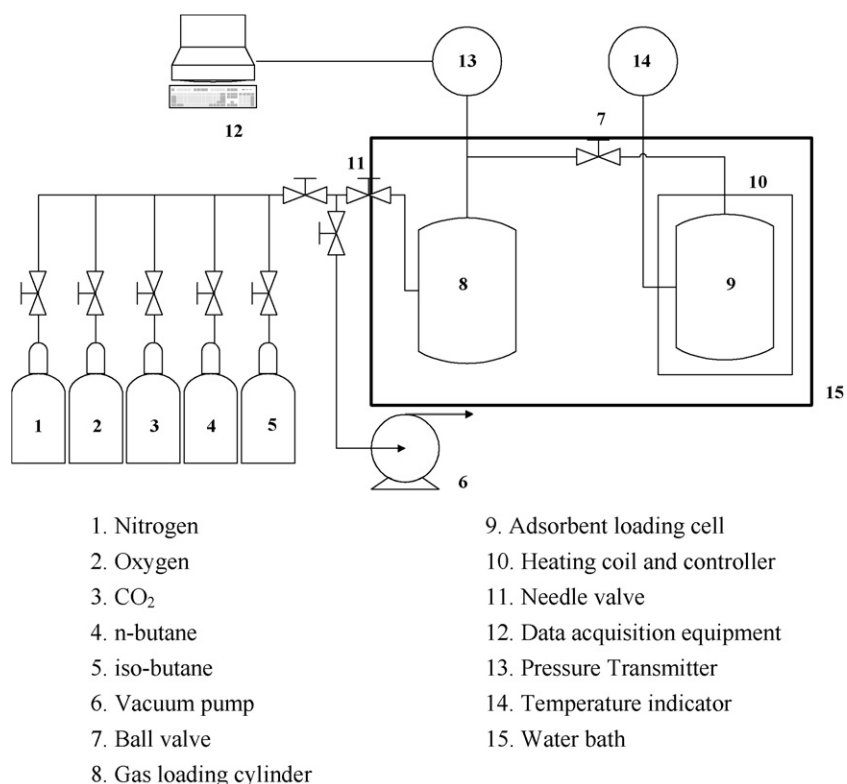


Fig. 2. Schematic drawing of static volumetric adsorption apparatus.

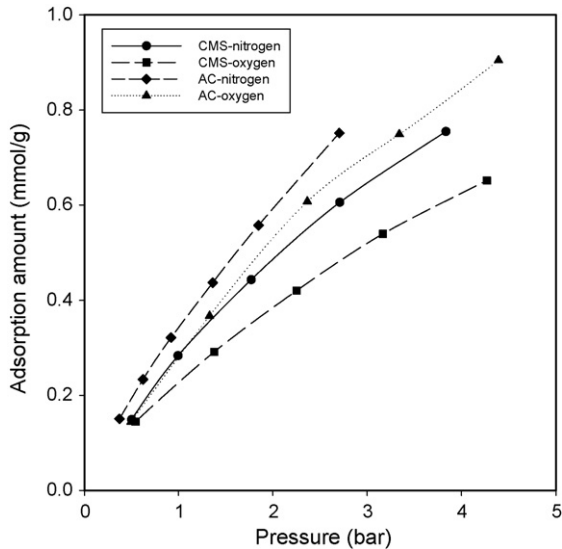


Fig. 3. Adsorption isotherms of carbon molecular sieves and activated carbons.

4. Results and discussion

4.1. Adsorption isotherms

The adsorption isotherm of the manipulated samples and commercial carbon molecular sieves could be acquired through the volumetric adsorption method. Fig. 3 shows the adsorption isotherms of the commercial carbon molecular sieves and activated carbons for pure nitrogen and oxygen. It is remarkable that the equilibrium adsorption amount of nitrogen and oxygen is not much different. Therefore, the separation in the pressure swing adsorption process does not depend on adsorption equilibrium and mainly depends on the adsorption kinetics. Compared to the commercial carbon molecular sieves, activated carbon has superior adsorption capability and has potentials to be selective carbon adsorbents by post-treatment process such as chemical vapor deposition. For example, the difference of adsorption amounts of nitrogen between on the commercial CMS and produced activated carbon is 20%, and that of oxygen is 35% at 1 bar. The difference between the two will be strong as pressure goes up.

Figs. 4 and 5 show oxygen and nitrogen adsorption isotherms of manipulated samples at heating rate of 10 °C/min and laminar flow condition. The adsorption amount obviously decreases along the increase of the treating time. Adsorption amount of oxygen and nitrogen in Figs. 4 and 5 have sudden decrease along the increase of the treating time. This can be explained that micropores on the activated carbon are narrowed along the increase of the treating time. Pore size control in this way gives more diffusion resistance in nitrogen diffusion than that in oxygen case. The kinetic diameter of nitrogen (3.64 Å) is larger than that of oxygen (3.46 Å).

The carbon deposition upon the pore mouth has not much influence on the adsorption amount. However, the excessive carbon deposition treatment can make the pore opening too narrow to adsorb the oxygen molecule and this may decrease the oxygen adsorption amount. The adsorption amounts of oxygen suddenly

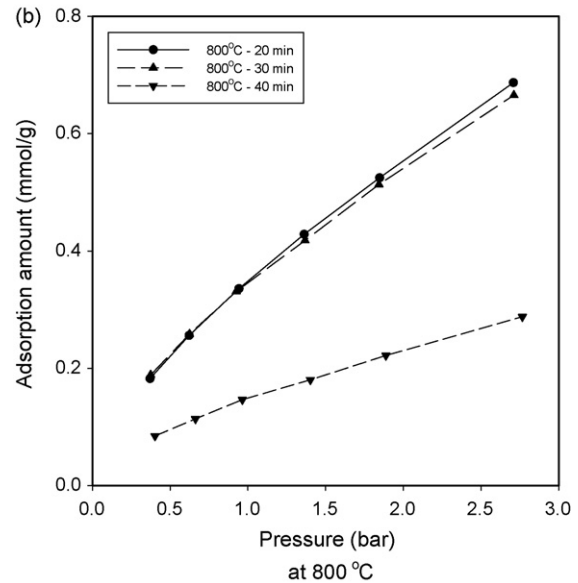
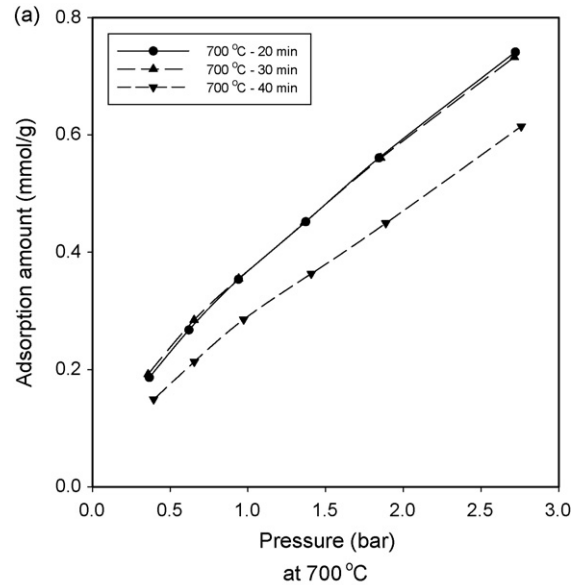


Fig. 4. O₂ adsorption isotherms of manipulated sample at 10 °C/min heating rate in laminar flow condition.

decrease while that of nitrogen decreases step by step relatively. The difference of adsorption amount of 20 and 30 min is smaller for oxygen than nitrogen. Because the kinetic size of oxygen is smaller than that of nitrogen, the adsorption amount of oxygen is retained more than that of nitrogen until the pore size is sufficiently small.

4.2. Diffusivity and selectivity of a manipulated sample

To separate nitrogen and oxygen, carbon adsorbents should have selectivity and it comes from the difference in adsorption velocity. Figs. 6 and 7 show the diffusion rate to the CMS of oxygen and nitrogen. Oxygen is adsorbed rapidly while nitrogen exhibits a relatively slow adsorption. During long-time diffusional uptake in Fig. 7, the fractional uptake of nitrogen

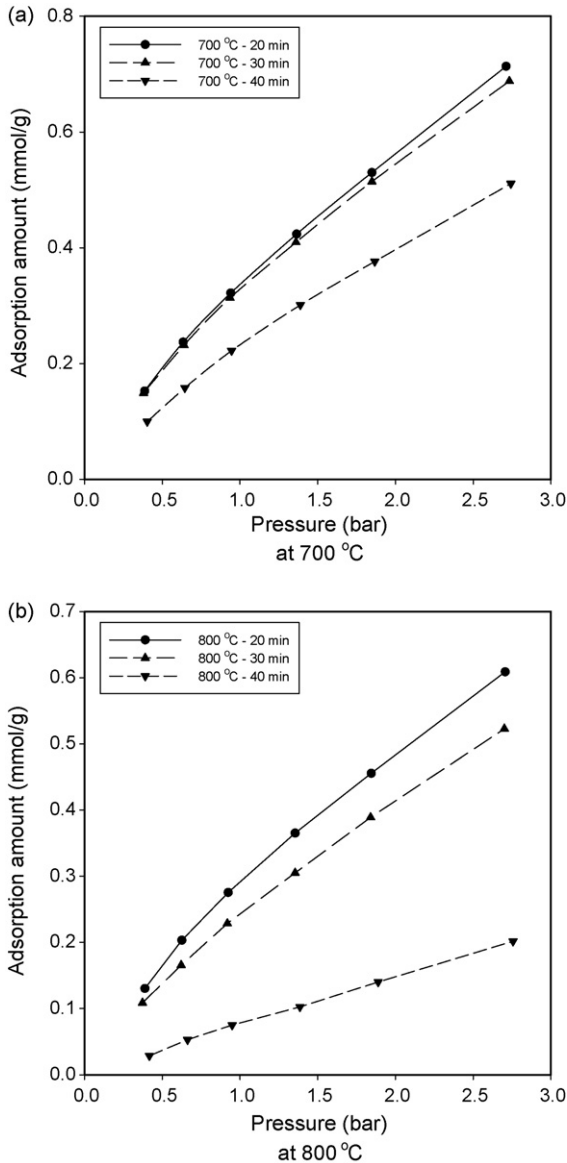


Fig. 5. N_2 adsorption isotherms of manipulated sample at $10^\circ\text{C}/\text{min}$ heating rate in laminar flow condition.

yields almost linear tendency. In the initial uptake curve, oxygen diffuses rapidly on the carbon molecular sieves and this adds selectivity.

We tried about 40 samples and only a few samples have a satisfactory selectivity for separation of nitrogen and oxygen. Figs. 8 and 9 show the diffusion characteristics related to the samples treated under the conditions of 700°C , $10^\circ\text{C}/\text{min}$, 40 min in laminar atmospheric flow and 800°C , $10^\circ\text{C}/\text{min}$, 30 min in turbulent atmospheric flow. These results were summarized in Table 2. In Table 2, the selectivity is defined as the ratio of diffusivity of oxygen to that of nitrogen in this experiment. As shown in Figs. 8 and 9, and Table 2, the diffusivity on the treated sample and the selectivity is changed depending on the treating time. Although the diffusivity is decreased with the treating time, the separation efficiency increases with the selectivity because the decreasing amount of the diffusivity of oxygen

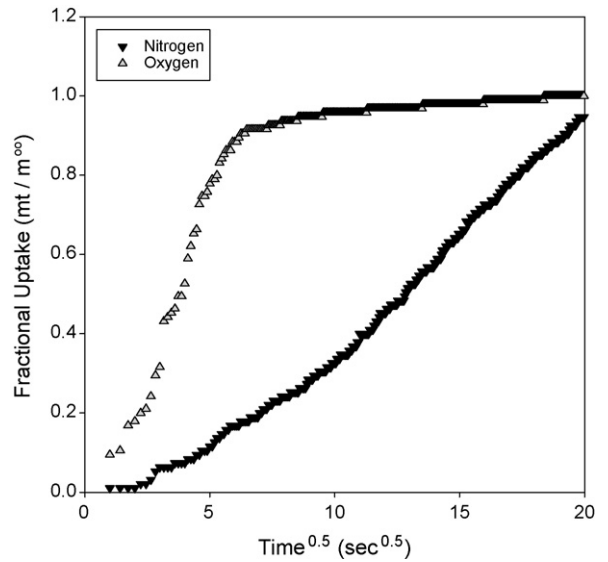


Fig. 6. Time dependent adsorptive behavior of carbon molecular sieves at short operation time.

is smaller than that of nitrogen with the treating time. Both of them have high selectivity over 20. Only in terms of selectivity, this is superior result than commercial carbon molecular sieves of which selectivity is 20 at 30°C .

4.3. Characteristics of benzene deposition on activated carbons

The deposition amount on the activated carbon increases with the treating time. After proper amount of deposition is done, extra carbon heap on the pore mouths will hinder entering of oxygen molecule. A key factor maybe is to stop heaping of heterogeneous carbon on the pore mouth at the proper treating time.

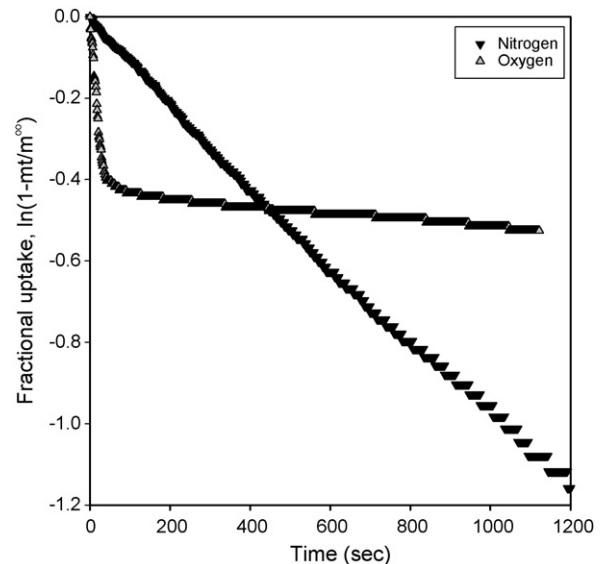


Fig. 7. Time dependent adsorptive behavior of carbon molecular sieves at long operation time.

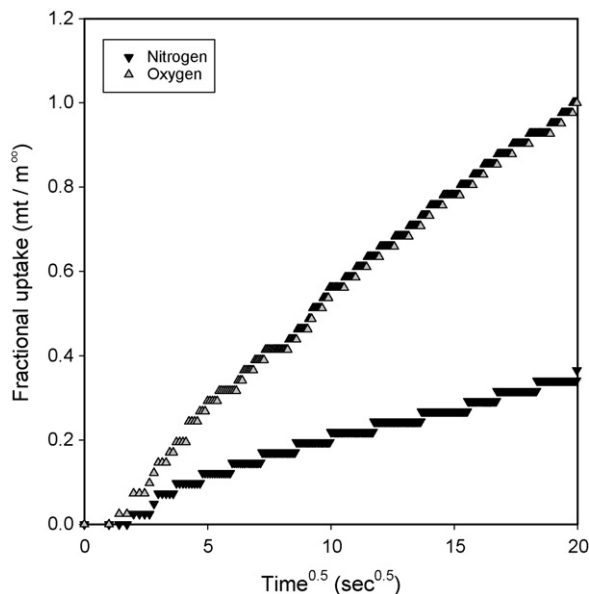


Fig. 8. Time dependent adsorptive behavior of treated samples under conditions at 10 °C/min, 700 °C, 40 min and laminar flow.

Samples treated in the high temperature region of 900 °C showed sudden pore clogging in deposition. It seems that fast piling on the pore mouth occurs in the high temperature region than in the low temperature region of 700 or 800 °C. That can be a defect in the deposition control, since it is difficult to stop deposition process in right time. In other words, slow deposition could be a preference for more accurate control. The heating rate does not have much influence on the pore size control and adsorption capacity of the already carbonized product. The retention time could be well explained in Fig. 10. Left side data group in Fig. 10 is from samples treated at 10 °C/min, and right side data group is from samples treated at 5 °C/min. Long retention in the furnace shortened oxygen capacity, but did not extend selectivity. In this result, the short retention time in the furnace is better than the long retention time.

Table 2
Comparisons of adsorption amount and selectivity under laminar and turbulent flow conditions

Peak temperature (°C)	Holding time (min)	D/r^2 (s ⁻¹)			Adsorption amount (ml/g) at 1 atm	
		Oxygen	Nitrogen	Selectivity	Oxygen	Nitrogen
700 (10 °C/min, turbulent flow)	30	0.0003152	5.64E-05	5.59	5.6487	5.8865
	40	0.0002454	3.25E-05	7.56	5.8662	3.2150
	50	0.0003396	4.28E-05	7.93	5.8374	5.1078
800 (10 °C/min, turbulent flow)	20	0.0001629	3.39E-05	4.80	4.0698	2.7207
	25	0.0005311	5.72E-05	9.28	2.5648	2.5261
	30	0.0004531	1.55E-05	29.31	2.7892	1.1943
700 (10 °C/min, laminar flow)	20	0.0003407	2.51E-05	13.60	9.3657	8.5097
	30	0.0003086	3.14E-05	9.83	9.3837	8.3328
	40	0.0003360	1.56E-05	21.52	7.2957	5.8426
800 (10 °C/min, laminar flow)	20	0.0003071	2.92E-05	10.52	8.8583	7.4127
	30	0.0002820	1.83E-05	15.39	8.8951	6.1883
	40	0.0002971	1.48E-05	20.12	3.7718	1.9662

Selectivity: diffusivity ratio (oxygen/nitrogen).

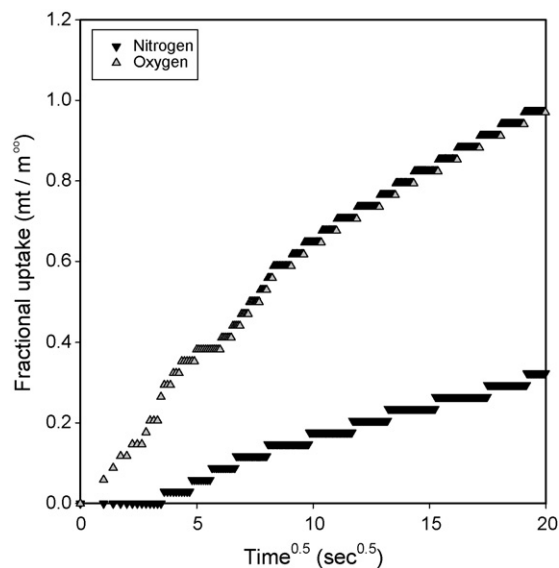


Fig. 9. Time dependent adsorptive behavior of treated samples under conditions at 10 °C/min, 800 °C, 30 min and turbulent flow.

Flow conditions were turbulent flow whose Reynolds number is 5300 and laminar flow whose Reynolds number is 1000. In the summary of Table 2, samples treated under laminar flow condition have better results than those treated under turbulent flow condition. Under laminar flow condition, the decrease of oxygen adsorption capacity is somewhat less than samples treated under turbulent flow condition. The laminar flow might give sufficient time for decomposition to be introduced on the pore mouth, not inside of the pore. However, strong flow may penetrate into the pore in turbulent condition. As a result, the reduction in oxygen adsorption capacity without improving selectivity could occur.

4.4. Pore size distribution in treated activated carbon

The tendency in the pore size reduction by chemical vapor deposition can be well exhibited by the BET method. Figs. 11 and 12 present the micropore distribution of activated

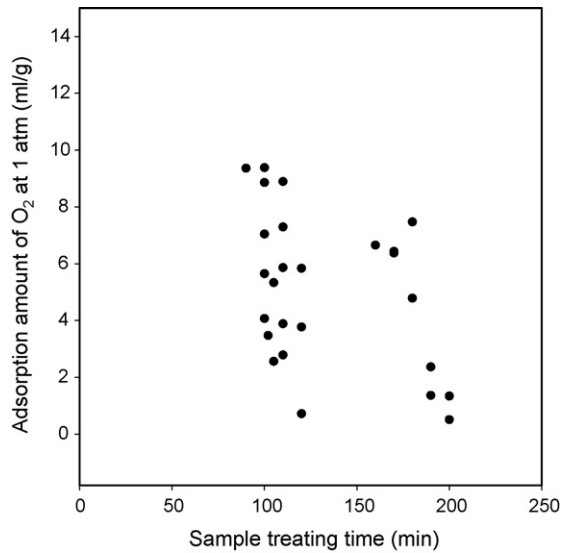


Fig. 10. Relationship between sample treating time and adsorption capacity of oxygen.

carbon and treated samples for 20 min and 30 min at 800 °C. The results show the effect of retention time on pore diameter. Average pore diameters are 2.57 Å for sample of 20 min at 800 °C and 2.43 Å for sample of 30 min at 800 °C, respectively. Both the pore sizes and pore volume decrease with the treating time. It is due to the blocking of pore mouth by the CVD method. Although the adsorption becomes relatively slow as shown in the previous Figs. 6, 8 and 9 because of these small and narrow pore size distribution, this distribution could lead to the high selectivity of oxygen to nitrogen in adsorption process.

Fig. 13 shows the adsorption amount of CO₂ (3.3 Å), *n*-butane (4.3 Å), *iso*-butane (5.0 Å) on the treated samples. Experiments were taken over samples treated under laminar flow condition at 700 °C, because the sample treated at 700 °C has bigger pore size than the sample at 800 °C and clearly shows the effect of pore size on adsorption amounts of used gas molecules—CO₂,

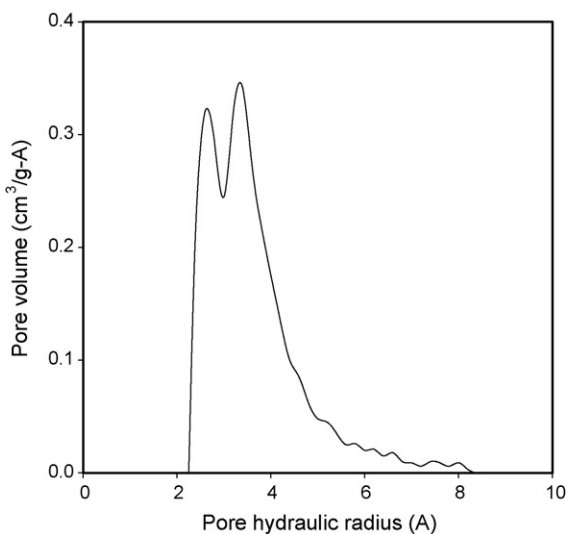


Fig. 11. Micropore region of activated carbon by BET method.

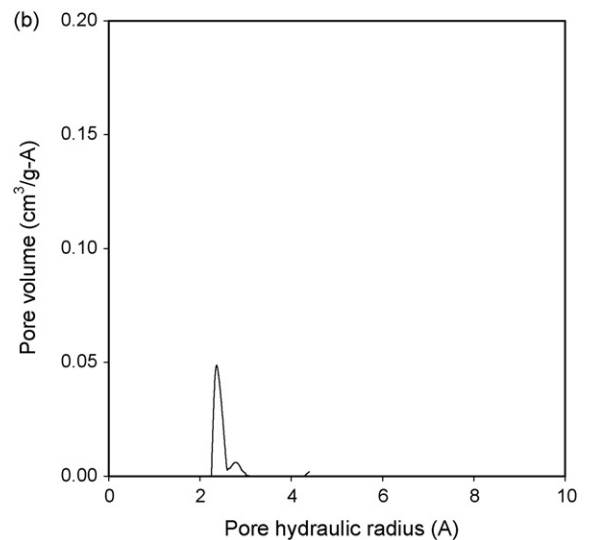
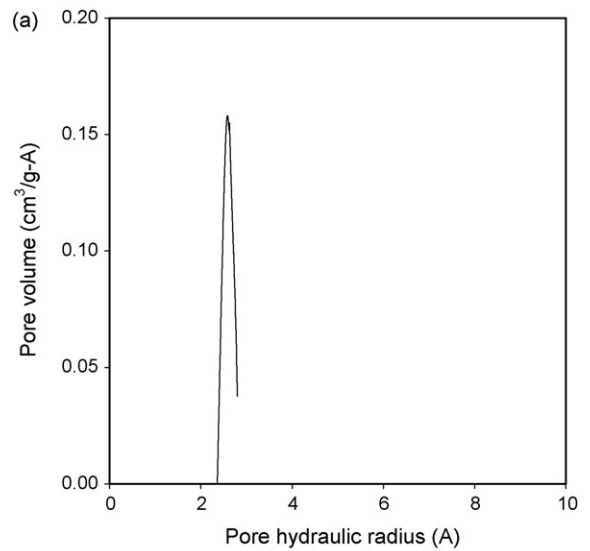


Fig. 12. Micropore region of treated samples by BET method.

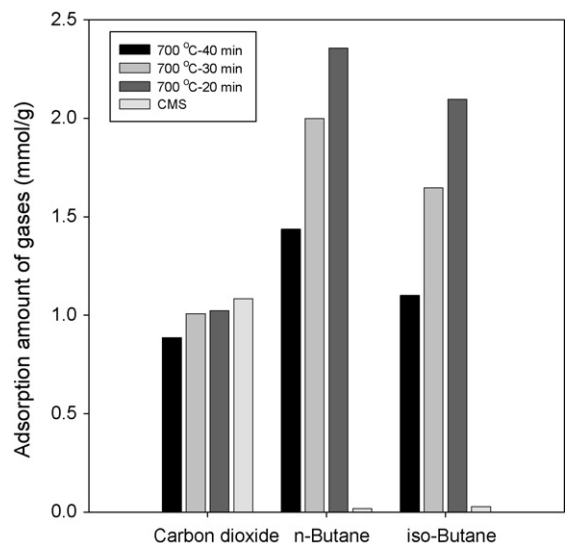


Fig. 13. Adsorbed amount of various gas molecules on the carbon adsorbents.

n-butane, *iso*-butane. As shown in Fig. 13, more deposition is carried out, the energy barrier blocking gas molecules are stronger. It is noticeable that the adsorption amount of CO₂ is almost same to four kinds of samples, which means that pores are not constricted under 3.3 Å. In other words, energy barrier blocking to diffuse through the pore for CO₂ molecules is almost of same level in these samples. When CO₂ diffuses into the micropore opening, gas molecule will transcend a lower activation barrier and the repulsive forces will be lower than the case of *n*-butane or *iso*-butane. As a result, CO₂ adsorption will be faster than *n*-butane or *iso*-butane adsorption. On the other hand, the adsorption amount of *n*-butane (4.3 Å) and *iso*-butane (5.0 Å) were diverse with treating time. It means that the diffusion of those molecules is constricted at these pore sizes. The energy barrier to *n*-butane (4.3 Å) and *iso*-butane (5.0 Å) molecules in commercial carbon molecular sieves is higher than others. It can be described that the pore size distributions of carbon molecular sieves are surprisingly unique. Because of these factors, the effective diffusivities of gases with different kinetic diameters are indicative of the pore opening sizes in microporous carbon adsorbent samples. In this way, the pore sizes will be measured indirectly by the selective adsorption of carbon adsorbents and this could be a more accurate way than BET measurement in observing the microporosity as shown in some previous researches [17–19].

5. Conclusions

In the experiment, chemical vapor was deposited on the activated carbon to adjust pore sizes on the adsorbent surface. Experiments were carried out to add selective property to carbon adsorbents, and turned out that adsorption characteristics can be improved by proper treatment.

1. Adsorption properties of activated carbon can be improved by proper post-treatment. Activated carbons were adjusted in the temperature region of 700 °C, 800 °C and 900 °C. At 900 °C, too fast deposition on the surface made the carbon adsorbents useless.
2. The heating rates of samples were 5 °C/min and 10 °C/min. Low heating rate narrows average pore size and decreases adsorption capacity, but chemical vapor deposition has stronger effect on control pore size.
3. Laminar flow condition was preferred to turbulent flow. Selectivity was improved in both conditions, but adsorption capacity treated in turbulent flow conditions was decreased severely. These results could explain that organic materials can easily diffuse into pores under turbulent condition and adsorption capacities diminish with heaped carbon.
4. Pore size distribution investigated by adsorption of CO₂ (3.3 Å), *n*-butane (4.3 Å), *iso*-butane (5.0 Å) assured the pore constriction and heightened energy barrier on the pore opening. Pore size distribution by BET method also showed that chemical vapor deposition narrowed pores and improved the selectivity of target gas from air.

Acknowledgement

This study was supported by a Korea University Grant.

References

- [1] T. Zhang, W.P. Walawender, L.T. Fan, Preparation of carbon molecular sieves by carbon deposition from methane, *Bioresour. Technol.* 96 (2005) 1929–1935.
- [2] A.L. Cabrera, J.E. Zehner, C.G. Coe, T.R. Gaffney, T.S. Farris, J.N. Armor, Preparation of carbon molecular sieves: two-step hydrocarbon deposition with a single hydrocarbon, *Carbon* 31 (1993) 969–976.
- [3] D. Lozano-Castello, J. Alcaniz-Monge, D. Cazorla-Amorós, A. Linares-Solano, W. Zhu, F. Kapteijn, J.A. Moulijn, Adsorption properties of carbon molecular sieves prepared from an activated carbon by pitch pyrolysis, *Carbon* 43 (2005) 1643–1651.
- [4] V.C. Geiszler, W.J. Koros, Effect of polyimide pyrolysis conditions on carbon molecular sieve membrane properties, *Ind. Eng. Chem. Res.* 35 (1996) 2999–3003.
- [5] M.J. Lazaro, J.V. Ibarra, R. Mo, K.M. Thomas, The release of nitrogen during the combustion of coal chars: the role of volatile matter and surface area, *Fuel* 75 (1996) 1014–1024.
- [6] P.J.M. Carrott, I.P.P. Cansado, M.M.L. Ribeiro Carrott, Carbon molecular sieves from PET for separations involving CH₄, CO₂, O₂ and N₂, *Appl. Surf. Sci.* 252 (2006) 5948–5952.
- [7] M.M.A. Freitas, J.L. Figueiredo, Preparation of carbon molecular sieves for gas separations by modification of the pore sizes of activated carbons, *Fuel* 80 (2001) 1–6.
- [8] Y. Kawabuchi, S. Kawano, I. Mochida, Molecular sieving selectivity of active carbons and active carbon fibers improved by chemical vapour deposition of benzene, *Carbon* 34 (1996) 711–717.
- [9] S. Villar-Rodil, R. Navarrete, R. Denoyel, A. Albiniak, J.I. Paredes, A. Martínez-Alonso, J.M.D. Tascon, Carbon molecular sieve cloths prepared by chemical vapour deposition of methane for separation of gas mixtures, *Microporous Mesoporous Mater.* 77 (2005) 109–118.
- [10] Z. Hu, E.F. Vansant, Carbon molecular sieves produced from walnut shell, *Carbon* 33 (1995) 561–567.
- [11] C. Nguyen, D.D. Do, Preparation of carbon molecular sieves from macadia nut shells, *Carbon* 33 (1995) 1717–1725.
- [12] Y.K. Kim, H.B. Park, Y.M. Lee, Preparation and characterization of carbon molecular sieve membranes derived from BTDA–ODA polyimide and their gas separation properties, *J. Membrane. Sci.* 255 (2005) 265–273.
- [13] R. Arriagada, G. Bello, R. García, F. Rodríguez-Reinoso, A. Sepúlveda-Escribano, Carbon molecular sieves from hardwood carbon pellets: the influence of carbonization temperature in gas separation properties, *Microporous Mesoporous Mater.* 81 (2005) 161–167.
- [14] Y. Kawabuchi, C. Sotowa, M. Kishino, S. Kawano, Chemical vapor deposition of heterocyclic compounds over active carbon fiber to control its porosity and surface function, *Langmuir* 13 (1997) 2314–2317.
- [15] Y. Kawabuchi, M. Kishino, S. Kawano, D.D. Whitehurst, Carbon deposition from benzene and cyclohexane onto active carbon fiber to control its pore size, *Langmuir* 12 (1996) 4281–4285.
- [16] D.M. Ruthven, N.S. Raghavan, M.M. Hassan, Adsorption and diffusion of nitrogen and oxygen in a carbon molecular sieve, *Chem. Eng. Sci.* 41 (1986) 1325–1332.
- [17] L.J. Wang, F.C.N. Hong, Surface structure modification on the gas separation performance of carbon molecular sieve membranes, *Vacuum* 78 (2005) 1–12.
- [18] R.K. Mariwala, H.C. Foley, Evolution of ultramicroporous adsorptive structure in poly(furfuryl alcohol)-derived carbogenic molecular sieves, *Ind. Eng. Chem. Res.* 33 (1994) 607–615.
- [19] I. Mochida, S. Yatsunami, Y. Kawabuchi, Y. Nakayama, Influence of heat-treatment on the selective adsorption of CO₂ in a model natural gas over molecular sieve carbons, *Carbon* 33 (1995) 1611–1619.